RESEARCH ARTICLE

An experimentally validated model for predicting the tensile modulus of tubular biaxial and triaxial hybrid braids

Ghazal Ghamkhar[1,2] | Majid Safar Johari[2] | Hossein Hosseini Toudeshky[3] | Mahdi Bodaghi[1]

[1]Department of Engineering, School of Science and Technology, Nottingham Trent University, Nottingham NG11 8NS, UK

[2]Department of Textile Engineering, Amirkabir University of Technology, Tehran, Iran

[3]Department of Aerospace Engineering, Amirkabir University of Technology, Tehran, Iran

Correspondence
Mahdi Bodaghi, Department of Engineering, School of Science and Technology, Nottingham Trent University, Nottingham NG11 8NS, UK.
Email: mahdi.bodaghi@ntu.ac.uk

Abstract

Braiding is a versatile and cost-effective approach to generating various composite structures for mechanical, sports, and biomedical engineering applications, which are different from each other. For example, a stent is a braided structure and blood penetration in it is essential as much as the right function. Predicting the tensile responses is a prerequisite for the success of implementation of braided structures, and it is usually performed via destructive mechanical testing that might be costly and/or time-consuming. Therefore, it is essential to provide a model that can accurately predict the tensile modulus. In this research, a theoretical model is developed using the simplification of a braided structure and is validated via testing of biaxial and triaxial braids composed of polyester, glass, and basalt yarns on a 16-carrier vertical braiding machine. Experimental results not only are used for the model validation but also show the effectiveness of axial yarn presence, hybridization, and the presence of high-performance yarn in the braided structures on the tensile properties. A good correlation between theoretical values and experimental results is observed approving the high accuracy of the proposed model. This paper is likely to fill a gap in the state of the art and provide pertinent results that are instrumental in the design of hybrid-braided structures with minimum computational/experimental effort. The research innovation centers on the use of two different yarns to make hybridization, simplicity of the model to be used for biaxial and triaxial braided structures, and a start to omit destructive tests.

KEYWORDS
biaxial braid, hybrid braid, tensile modulus, theoretical model, triaxial braid, tubular braid

1 | INTRODUCTION

Designing structures with proper performance, especially fiber-reinforced composite materials, requires familiarity with the mechanical behavior of materials in different conditions. Tensile modulus is one of the most important mechanical properties in determining the tensile performance of these structures. Tensile properties of fiber-reinforced composite materials investigated in different studies.[1–4] These papers show

that this issue has become more important in the last 10 years.

Braided structures can be used as a reinforcement in a composite material. A braided structure is created by the intertwining of two strands of yarn in opposite directions at an angle θ. It seems that not much effort has been made over the years to investigate tensile properties of braid structures, model and predict the tensile properties of this structure.

Probably the first research on the braided structure by Branchweiler[5] was done in 1954 on the tensile and structural properties of biaxial braids. In addition, a method of tensile test on the tubular braids was introduced by him. Phoenix[6] conducted a study on braids containing an elastic core and found that the tensile modulus of the braid's components is one of the most important parameters affecting the mechanical proper-ties of the braid structure.

Hristov et al.[7] suggested a model for predicting the tensile properties of hybrid biaxial braids by using the energy method. In his study, braids specimens were produced on a 16-carrier vertical braiding machine at 12°, 25°, and 36° braiding angles. The results of this study indicate that the model proposed by Hristov is able to successfully calculate the rupture force of the braids. In addition, the results of this study showed that increasing the braiding angle leads to a reduction in force to the point of rupture and a significant increase in elongation. This is because as the braiding angle increases and the yarns move away from the braiding axis, less force is required to pull the braiding.

Rawal et al.[8] investigated the structural tension of the braid examined a simple analytical tension model based on the geometry, kinematics, and properties of the monofilaments. The results showed that under tensile force, the deformation of the geometric occurs in the braid structure. It was assumed that the shape and diameter of the filaments remain unchanged during stretching and the minimum average distance between them can be calculated by the Peirce model. In order to validate the model, braid samples were produced using polypropylene monofilaments on a 16-carrier braiding machine with a rotational speed of 16.49 radians per second and a braiding speed of 0.61 cm/s were evaluated. There was a very good agreement between the experimental and theoretical results. In addition, the nonlinear behavior of the braid in axial loading mode was observed.

Dabiryan and Johari[9] investigated the tensile properties of tubular braids using the energy method. This study showed that the tubular braid's reaction to tensile could be studied in two stages. In the first stage, the deformation of the braid structure geometric occurs and its geometry deforms to a jamming state. In the jamming mode,

maximum geometric deformation has occurred and there is no more space to move the yarns that make the braid. In this stage, the stress–strain diagram has a slight slope. As the tension continues, the mechanical reaction of the yarns forming the braid occurs as the second step. This step is accompanied by stretching, bending, and compression of the braid yarns. This gradually increases the braid modulus and increases the slope in the stress–strain diagram. The mechanical properties of the yarns that make up the braid play a major role. In addition to the above, this study led to the introduction of Equation (1) to calculate the tensile modulus of a braided structure:

$$E_{\mathrm{b}} = \frac{l_{\mathrm{ui}}\left(l_{\mathrm{y}}^2 \pi d_{\mathrm{y}}^2 E_{\mathrm{y}} \cos^2\alpha + 96 B_{\mathrm{y}} \sin^2\alpha\right)\cos^2\theta\cos^2\theta_{\mathrm{j}}}{2\pi l_{\mathrm{y}}^3 d_{\mathrm{y}}^2\left(\cos^2\theta + \cos^2\theta_{\mathrm{j}}\right)}. \quad (1)$$

In the above equation, l_{y}, l_{ui}, θ, θ_{j}, d_{y}, E_{b}, E_{y}, B_{y}, and α, are yarn length in the unit cell in term millimeters, unit cell length braid in term millimeters, braiding angle in normal in term degree, braiding angle in the jamming mode in term degree, yarn diameter in the unit cell (diameter of the yarns forming the braid) in term millimeters, tensile modulus (Young's modulus) in the braid structure in term centimeters per tex, The tensile modulus of the yarns forming the braid in term centimeters per tex, The bending rigidity of yarns of the yarns in term centimeters per tex, which is calculated by using B = EI, and the crimp angle of the braid yarns in term degree, respectively. The crimp angle depends on the parameters such as yarn diameters, number of carriers, and interlacing pattern (Interlacing the pattern of the yarns to produce a braided structure is known as a braid weave pattern. Diamond, regular, and Hercules are the most known the weave pattern of the braid). The value of the sine of this angle is obtained from the ratio of the yarn diameter to the length of the yarn in the unit cell of the braid structure.

Boris et al.[10] compared the tensile properties of biaxial and triaxial braids and proposed the theoretical models to predict the tensile modulus of these structures. The results of this study showed a stronger structure and better tensile properties of the triaxial braided structure than the biaxial braid. In addition, it was observed that by increasing the braiding angle from 13° to 20°, the tensile properties of both structures decrease. Their theoretical models also matched well with the experimental results obtained.

Zhang Yujing et al.[11] proposed a mathematical model by dividing a braid structure to four basic loops units. The results show that the tensile force of yarns and the fluctuating amplitude of the stress distributions in them are directly related to each other.

Afzali et al.[12,13] conducted research to determine the effect of fiber type and ratio on the tensile properties of the hybrid braid structures and their composites. Experimental studies and statistical analyzes in their research were performed on 15 different samples produced from different combinations of two and three pieces of PET, PP, and PA yarns. The results showed that the presence of the highest amount of PA fibers in such structures leads to higher tensile properties. In addition, the sample containing 75% PA yarn, 12.5% PP yarn, and 12.5% PET yarn showed the best performance among the samples of the hybrid braid composites.

Noghabi et al.[14] investigated the tensile behavior of cylindrical braids in both normal and composite states. In order to investigate the effect of the braid weave pattern, three types of braiding machines were used to produce samples with 1/1 (diamond), 2/2 (regular), and 3/3 (Hercules) designs. In addition, polyester yarn was used as a background yarn, and polyester and polypropylene yarns with different two grades were used to study the core effect. The results showed that the tensile strain and secondary modulus of the braids and composites reinforced with them are ascending by changing the pattern from 1/1 to 2/2 and decreasing from 2/2 to 3/3. The difference is that their values in composite samples have been significantly reduced. Because the modulus of polyester is higher than the modulus of polypropylene, the modulus of braids with polystyrene core is higher than the modulus of braids with a polypropylene core.

Ghaedsharaf et al.[15] Investigated the three-dimensional and internal geometry of biaxial braids produced according to patterns 1/1 and 2/2 using carbon fibers. They founded that not only did the friction between the fibers reach its maximum in the jamming state, but also the coefficient of friction had no significant effect on the jamming state. In addition, the results showed that changing the range of fiber elasticity modulus had no significant effect on the jamming state. Also in this study, a yarn containing its constituent filaments was modeled in a braid structure. The results compared with CT scans and confirmed the model.

Singh et al.[16] to optimize braided beam structures in frames of rail vehicles provided a combination of finite element (FE) and a genetic algorithm (GA) using variations in braiding angle and the number of layers. In this study, the composite samples were produced in 3–9 layers using Tenax E HTS40 F13 carbon fiber and RTM6 epoxy resin at the braiding angles of 30°, 35°, 40°, 45°, 50°, 55°, and 60°. An error of <3% of the results indicates the algorithms effectiveness implemented in this study in optimizing the design of individual composite components taking into account the performance of the whole structure.

Since the flexural and tensile modulus are related to each other. Knowing about the flexural modulus can also provide a good view of the tensile modulus. Masoumi et al.[17] evaluated the effect of intralayer hybridization on the flexural moduli of the triaxial braided composite lamina. That is, tubular braids are converted into flat forms and used. Four triaxially braided were produced on a circular braiding machine using carbon and basalt fibers as axial and braid yarns. Then, by using a vacuum bag using epoxy resin were turned into the composite lamina. Finally, a three-point bending test was carried out on specimens according to ASTM D790 in both longitudinal and transverse directions. Test results showed that a specimen with carbon fibers as axial yarns and basalt fibers as braid yarns and a specimen with carbon fibers as axial yarns and braid yarns have the same longitudinal flexural behavior. In addition, a specimen with basalt fibers as axial yarns and carbon fibers as braid yarns and a specimen with carbon fibers as axial yarns and braid yarns have the same transverse flexural behavior. It seems that hybridization is a proper method to reduce the cost of carbon composites without reducing their flexural performance.

Parameters such as random fiber arrangement, possible fiber modulus distribution, and voids have a significant effect on the mechanical performance of braided composites. Han et al.[18] predicted mechanical behavior of braided composites by considering stochastic characteristics. The results showed that the wider fiber modulus dispersion led to the earlier nonlinear behavior of braided composites.

Today, the use of braid structures in different industries such as reinforcement in composite materials, and tissue structures is increasing. Therefore, the mechanical properties of this structure such as tensile properties and internal geometry braided composites have been the subject of a large number of research works.[19–31] For example, Wang et al.[21] Studied the torsional properties of 3D braided composite shafts numerically and experimentally. The experimental results validated the FE model. Moreover, the damage observed on the surface progressed into the internal structure. Oguz Eryilmaz and Erhan Sancak[23] modified the epoxy resin to enhance interfacial adhesion between matrix and carbon fiber using APTES and APMDMS at different concentrations, then produced the carbon-braided composites by the vacuum-assisted resin infusion method. The results showed that using APTES in the epoxy resin led to higher mechanical properties of braided composites than APMDMS at the same concentration. In addition, they reported that 0.5% was an ideal concentration of treater material. Zahabi et al.[28] investigated the thermal properties of a three-dimensional braid composite under dry

and seawater conditions. The statistical analysis of the results revealed the friction coefficient of all composites with increasing load and sliding speed in dry and seawater conditions raised and decreased, respectively.

The use of different yarns and fiber in a braided structure leads to improving the structural properties and characterization. This structure is known as a hybrid braid. Due to the presence of more than one type of yarn in a hybrid braid, which is macroscopically distinguishable, the hybrid braid can be considered a kind of advanced composite material. The models presented in previous research works required the calculation of many parameters that were highly sensitive. In addition, calculation of these parameters needed performing destructive tests sometimes. A simple and high-precision theoretical model to predict the tensile modulus of hybrid braids is a real need. In this work, we develop a theoretical model for predicting the modulus of the biaxial and triaxial hybrid braided structures without computational complexity and performing destructive tests. For this novelty, the complex braid structure is first equated with a simple structure, then the equations and required parameters are developed. For model validation, five different samples are fabricated and tested mechanically in a tensile mode. A good correlation is observed between experimental and theoretical results showing the high accuracy of the model. Other innovations of this research include the use of two different yarns in terms of performance to produce the hybrid braids, the simplicity of the theoretical model, the ability to use the model for biaxial and triaxial braided structures, and omitting destructive tests. Due to the lack of any similar model and results, it is expected that the results and model supplied in the present work would be instrumental towards a reliable design of hybrid-braided structures with minimum computational/experimental efforts. Therefore, in summary, it can be said that the novelty of this work relates to using of different yarn types that have various tensile properties to make a hybrid braid and simple modeling to predict the tensile properties of the braid. Due to the complex structure of braid and the importance of reinforcing properties in composites, this manuscript just focuses on dry braid to highlight its related issues as part one. We hope to study braid-reinforced composites in the future and in other parts.

2 | EXPERIMENT

To obtain the aim of this work, to compare the experimental and theoretical results a model validation is necessary. The production of the samples and a tensile test were done in this section.

2.1 | Materials

In this work, polyester, E-glass, and basalt yarns were used to supply the braid samples. The tensile load of the polyester, E-glass, and basalt yarns was characterized by using an Instron 5566, consistent with the ASTM D 578 and the ASTM D 2256.[32,33]

The obtained characteristic as the yarns' properties were indexed in Table 1.

2.2 | Manufacturing the two-dimensional hybrid braids

Five different two-dimensional biaxial and triaxial tubular hybrid braids structures were manufactured according to the experimental plan as shown in Table 2.

As can be seen in Table 2, the coding of the samples is done in three parts. The first part shows that the structure of the braid is biaxial or triaxial, marked with B or T letters, respectively. To show different combinations in biaxial braids, a number is placed next to the letter B. The middle part indicates the type of axial yarn used. The letters B, G, and N mean basalt, glass, and without axial yarn, respectively. The last section also shows the braiding angle, which is equal to 40° in all samples. In all these samples, the braid structure includes 16 yarn strands. Therefore, the effect of the axial yarn's type is determined by comparing samples T-B-40 and T-G-40 and keeping constant the braiding angle, kind, and the number of yarn strands. Moreover, the effects of the braid yarn's type and its combination had determined by comparing samples B1-N-40 to B3-N-40. It is necessary to mention that B1, B2, and B3 refer to the braid structures containing 12, 8, and 4 polyester yarn strands, respectively.

Figure 1 The lateral surface of the braid structure at a 40° angle.

As can be seen, there is almost no space for the yarns to move during stretching and can be said that the braid is in the jamming position or close to the jamming. The braiding angle affects the tensile properties of the braid, and the selection of a 40° angle eliminates the need to calculate the jamming angle in the development of the theoretical model and can be ignored change the braiding angle during the tensile process.

The tubular hybrid braid structures were produced on a 16-carrier vertical braiding machine including eight

TABLE 1 Properties of the yarns used

Type of yarn	Yarn count (Tex)	Maximum load (N)	Strain	True stress (cN/Tex)	Density (g/cm^3)
Polyester	256	120.67	0.189	40.105	1.38
Basalt	778	374.88	0.0269	48.185	2.7
E-Glass	600	247.01	0.0197	41.168	2.55

TABLE 2 The experimental plan

Braid code	The number and the type of braid yarns	Braiding angle (°)	Structural axis	Type of axial yarns
T-B-40	16-Polyester	40	Triaxial	Bazalt
T-G-40	16-Polyester	40	Triaxial	Glass
B1-N-40	12-Polyester/4-bazalt	40	Biaxial	–
B2-N-40	8-Polyester/8-bazalt	40	Biaxial	–
B3-N-40	4-Polyester/12-bazalt	40	Biaxial	–

FIGURE 1 The lateral surface of the braid structure

axial yarn feeders. This braiding machine is shown in Figure 2.

2.3 | Tensile tests

The tensile test of specimens is carried out to obtain the tensile modulus of them by SANTAM tensile tester at 25 ± 2°C temperature and 65% ± 5% relative humidity. The test speed and the gauge length are 75 mm/min and

FIGURE 2 The 16-carrier vertical braiding machine

250 mm, respectively. Each of the braid samples is tested five times and the average of them is reported as the result of a sample.

According to the placement of the braid structure in the tensile test machine shown in Figure 3, the length of each braid is 120 cm. After being placed in the appropriate jaws of the tensile test, the distance between the two jaws at the beginning of the tensile test (gauge length) is 25 cm.

3 | THEORETICAL MODEL

In the current work, presenting the model to predict the tensile modulus of tubular biaxial and triaxial hybrid braids is achieved by performing the following three steps:

3.1 | Equivalence of complex structure with a simple structure

In the first stage, the structure of the biaxial and triaxial tubular braids was simplified. A braided structure
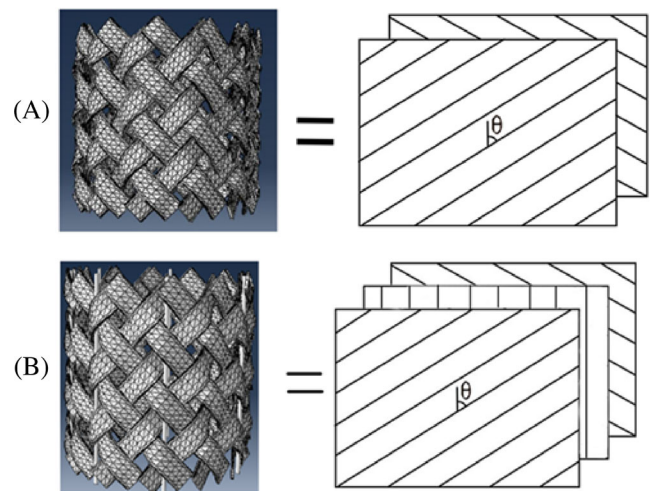

FIGURE 4 (A) Simplification of biaxial tubular braids. (B) Simplification of triaxial tubular braids

consists of the interlacing yarns, which are passed under and over each other. The interlacing yarns in each direction, form a single layer. Therefore, it can be stated that a biaxial braid is a two-layer laminate consists of single-sided yarns with angle θ. If there are axial yarns in the braid structure, another batch of yarns is placed directly between the interlacing yarns and a triaxial braid is a three-layer laminate. Simplification of biaxial and triaxial tubular braids is shown in Figure 4A,B, respectively.

Therefore, in the current work, a tubular biaxial hybrid braid is considered a laminate or ply with two layers that is made of a combination of two different yarns that are recognizable on a macroscopic scale. In a similar way, a tubular triaxial hybrid braid is considered as a laminate or ply with three layers that are recognizable on a macroscopic scale. Because the definition of composite applies to this structure, the rules, equations, and relationships governing composites about this laminate are also usable.

3.2 | Development of equations

Equation (2) is one of the well-known equations in macro mechanics used to calculate the tensile modulus in a representative volume element of a ply composite, which contains a fiber (Figure 5).[34]

Where E_{11}, V_f, E_f, V_r, and E_r are the tensile modulus of representative volume element in 1 direction, the volume fraction of fiber or yarn, the tensile modulus of fiber or yarn, the volume fraction of resin, the tensile modulus of resin, respectively.

In the second stage, Equation (2) is the basis and is rewritten according to the simplified structure as follows:
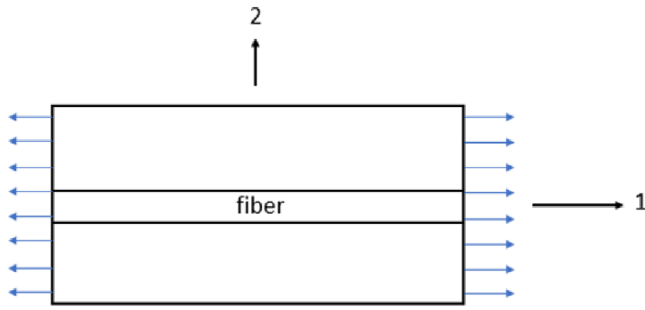
FIGURE 5 A representative volume element

$$E_{11} = V_f E_f + V_r E_r, \qquad (2)$$

Since the simplified layers according to Section 3.1 contain different yarns in different directions and no resin has been applied to them. On the other hand, according to Figure 4A,B, the amount of force applied in the direction of 1 and then the amount of tensile modulus is also related to the cosine of the braiding angle. Therefore, Equation (2) is written in the form of Equation (3) for a biaxial hybrid braid.

$$\begin{aligned} E_{11} &= \cos\theta \times V_{f1} \times E_{f1} + \cos\theta \times V_{f2} \times E_{f2} \\ &= \cos\theta \times (V_{f1}E_{f1} + V_{f2}E_{f2}), \end{aligned} \qquad (3)$$

where V_{f1}, E_{f1}, V_{f2}, E_{f2}, and θ are the volume fraction of basalt yarn, the tensile modulus of basalt, the volume fraction of Polyester, the tensile modulus of polyester, and braiding angle, respectively.

In a triaxial hybrid braid that the two outer layers contain one yarn, and the middle layer is composed of another yarn. The axial yarns in triaxial braid are parallel to the braiding axis. Therefore, the braiding angle will be zero degree and Equation (2) is written in the form of Equation (4) for a triaxial hybrid braid.

$$E_{11} = \cos\theta \times V_{f1} \times E_{f1} + V_{f2}E_{f2}, \qquad (4)$$

where V_{f1}, E_{f1}, V_{f2}, E_{f2}, and θ are the volume fraction of polyester yarn in outer layers, the tensile modulus of polyester in outer layers, the volume fraction of axial yarns, the tensile modulus of axial yarns, and braiding angle, respectively.

Given that most of the structure of a tubular braid is empty space, practically the axial yarns in the middle layer are effective. However, it should be noted that the presence of the two outer layers keeps the yarns in the middle layer and their effectiveness. Therefore, seems that the tensile modulus of triaxial braids is higher than biaxial braids with the same yarns.

3.3 | Parameters calculation

In the final stage, the parameters in the equations are calculated. According to Equations (3) and (4), these parameters are the tensile modulus of the yarns which are used and the volume fraction occupied by the yarns in a braid structure.

3.3.1 | Yarn tensile modulus

The tensile modulus is an important parameter to describe tensile behavior and defines mathematically as a ratio of tensile stress to tensile strain.

The tensile stress is the ratio of the tensile load applied to the surface. Therefore, about the complex structures such as braided structures it is better to consider the value of tensile true stress. Because accurate calculation of the area is difficult and is associated with errors. The true stress is presented in Table 1.

The tensile strain mathematically is the ratio of elongation to initial length. The Strain values for each yarn are listed in Table 1. As can be seen in Table 1, the strain values are very small compared to the true stress ones. Therefore, they have been omitted in the calculations.

3.3.2 | Volume fraction

The volume fraction values are calculated according to the density of the yarns which are listed in Table 1, Equations (5) to (8) and according to the processes which are shown in Figures 7 and 8 for biaxial and triaxial hybrid braids, respectively.

$$\frac{1}{\rho} = \frac{W_{f1}}{\rho_{f1}} + \frac{W_{f2}}{\rho_{f2}}, \qquad (5)$$

where ρ, ρ_{f1}, ρ_{f2}, W_{f1}, and W_{f2} are the braid density, the density of basalt or glass yarn, the density of polyester yarn, basalt or glass yarn weight fraction, and polyester yarn weight fraction, respectively.

$$V_{f1} = \frac{W_{f1}}{\rho_{f1}}\rho, \qquad (6)$$

$$V_{f2} = \frac{W_{f2}}{\rho_{f2}}\rho, \qquad (7)$$

W_{f1}, and W_{f2} are the ratio of the polyester weight in the braid to the braid weight, and the ratio of the glass or bazalt weight in the braid to the braid weight, respectively.
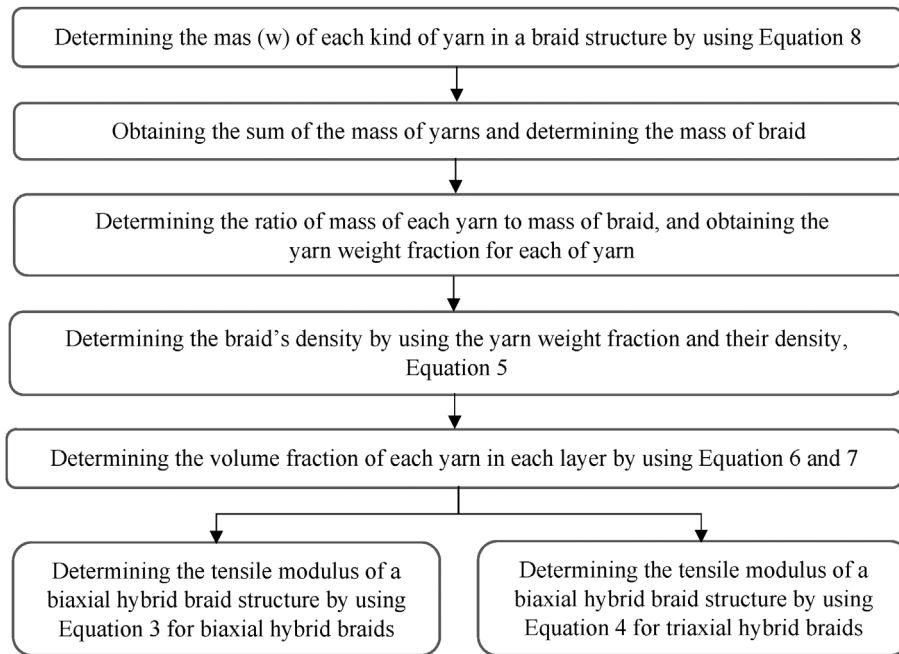
Determining the mas (w) of each kind of yarn in a braid structure by using Equation 8

↓

Obtaining the sum of the mass of yarns and determining the mass of braid

↓

Determining the ratio of mass of each yarn to mass of braid, and obtaining the yarn weight fraction for each of yarn

↓

Determining the braid's density by using the yarn weight fraction and their density, Equation 5

↓

Determining the volume fraction of each yarn in each layer by using Equation 6 and 7

↓

| Determining the tensile modulus of a biaxial hybrid braid structure by using Equation 3 for biaxial hybrid braids | Determining the tensile modulus of a biaxial hybrid braid structure by using Equation 4 for triaxial hybrid braids |

The weight of the braid is also the sum of the weights of the yarns obtained.

A braided structure is created by interlacing a number of yarns with a specified Tex count (mass of a 1000 m of yarn) at an angle of θ. The mentioned parameters affect the tensile properties and weight of the braid. In addition, by considering the units of the mentioned parameters and the unit of weight, Equation (8) can be used to calculate the weight of the yarn used in the braid structure:

$$w = (N \times T \times \cos\theta)/1000, \qquad (8)$$

where w is the mass of the yarn in terms of the gram, N is the number of a kind of yarn in a braided structure, T is the yarn count in terms of Tex, and θ is the braiding angle in terms of degree. As mentioned before this experimental equation used Tex count. Therefore, all of the specimens have the same total length.

It should be noted that the braid angle is equal to zero for axial yarns in the braid structure. Because these yarns are perfectly parallel to the braid axis in the structure. In general, the tensile modulus of biaxial and triaxial hybrid braids is according to the shown flowchart in Figure 6.

4 | RESULTS AND VALIDATION OF THE MODEL

4.1 | Experimental results

The force-extension diagram obtained from experimental tensile test of braid samples is shown in Figure 7.

The tensile force-extension behavior of the biaxial and triaxial hybrid braid structures can be explained in two and three stages, respectively. In the first stage, when the slope of the graph is low, the braid under tensile load undergoes geometric deformation to reach the jamming state. The slop of the triaxial hybrid braids is greater than the biaxial ones due to the strength caused by the presence of axial yarns. The second stage is associated with increasing tensile force and rupturing the braid. In the biaxial braids, there are several peaks in this part of the curve due to failed filaments in the braids. The number of these peaks will decrease by increasing the amount of yarn with higher tensile properties in the biaxial hybrid braid structures. These two stages are the same in the biaxial and triaxial hybrid braids. In biaxial hybrid braids, the second stage is the final stage because the braid is completely failed. While in triaxial hybrid braids, there is an additional stage where the braid has not completely broken but has lost most of its efficiency.

As mentioned before, a braid is a complex structure without a specific and measurable cross-section. Therefore, it is almost impossible to calculate the stress as the tensile force per cross-section. To avoid these complications, an attempt has been made to identify the sample with the best performance by comparing the loads and the extensions in different specimens. Therefore, according to Figure 7, the triaxial hybrid braids not only do not rupture in the beginning but also still resist against the tensile force after the final strength. However, this resistance is much less than the final resistance. First, the axial yarns which have less elongation, and more force are failed, then the force is borne by the polyester yarns,
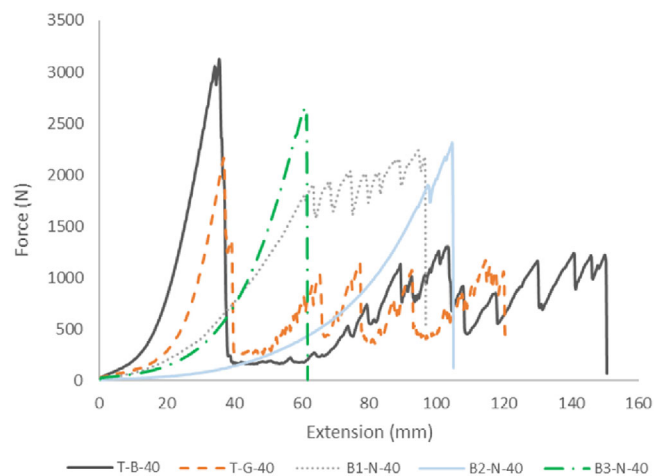
FIGURE 7 Force-extension diagram of the braid structures

FIGURE 8 The tensile modulus results in tubular hybrid braid

which are placed diagonally in the braid and have less force than glass or basalt. In addition, the increase in extension and force of the basalt-axis sample is greater than the glass-axis sample. Because the strength and elongation of glass yarn are less than basalt yarn. In biaxial hybrid braids, increasing the basalt yarn leads to increasing the strength. Because basalt yarn is more resistant than polyester yarn. These results are consistent with similar studies.[12–14] If the number of polyester yarns is much more than basalt yarn (B1-N-40), in the tensile behavior of the braid, instabilities are observed in the form of several peaks, which are eliminated by increasing the amount of basalt yarn. The basalt yarn is composed of several filaments, some filaments may be stretched during braiding which in combination with a large amount of polyester yarn will be more pressed and approached to jamming. Therefore, when the filaments of basalt yarn ruptured, for a moment the ability of the structure to withstand the tensile force decreases, but due to the presence of other yarns, the structure still has the ability to withstand the tensile force. The presence of equal amounts of basalt yarn and polyester yarn in the braid structure (B2-N-40) largely eliminates this problem. Due to the triaxial sample with eight axial basalt yarn has a higher force than the biaxial sample with 12 basalt yarns and eight polyester yarns, can be stated that the triaxial hybrid braid has a better function than the biaxial ones.

4.2 | Validation and modification of the model

The experimental tensile modulus values and those obtained from the model presented in Section 3 are listed in Table 3 and shown in Figure 8. In addition, SD or the
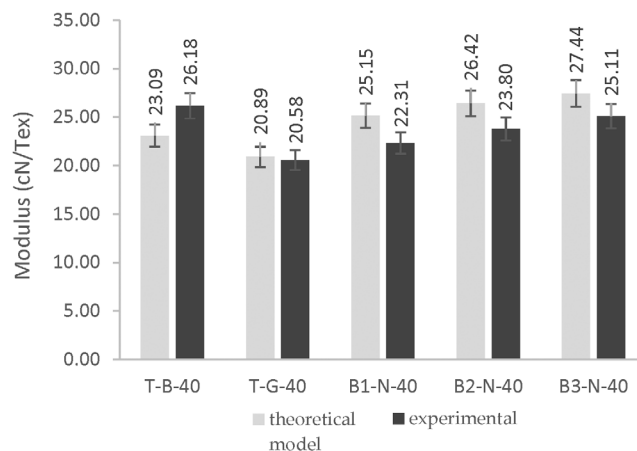
standard deviation tabulated in the Table. SD is the average amount of variability in your data set. It tells us, on average, how far each score lies from the mean. Therefore, SD has no unit.

It is necessary to mention it is not possible to accurately measure the effective cross-section of the braids experimentally, or with acceptable accuracy. Therefore, the engineering stress values are calculated by dividing the force values by the linear density of the braid structure in terms of Tex units. On the other hand, the cross-sectional area of the braid structure changes while tension is applied, and this causes the braiding angle and strain values will be changed. Therefore, it is necessary to convert engineering stress and engineering strain into their true values using appropriate equations. To avoid the effect of changes in strain and braiding angle during stretching, and also because of the elongation values are very small compared to the force values, the strain values are omitted in the calculations. Therefore, the engineering stress values are considered as the tensile modulus values.

As can be seen, the difference between the experimental results and the model predicted values is approximately 10–13 N. This difference is more than 40% in all kinds of samples.

A braided structure is a very complex structure, and the steps taken in Section 3 to predict the tensile modulus of two-dimensional hybrid braided structures were performed with some simplifications that can lead to the difference between the experimental results and the modeling. However, the following steps were taken to identify the sources of the errors:

1. Previous studies also referred in Section 1, were showed that the cosine of a braiding angle to power 2 is related to the tensile properties. Applying this,

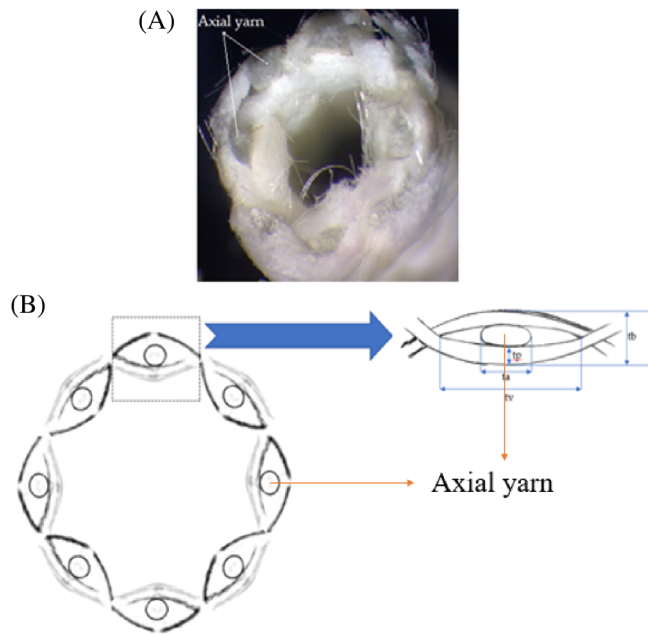| Braid code	The experimental value	The value obtained from the model	SD
T-B-40	26.18	39.52	0.51
T-G-40	20.58	34.96	0.70
B1-N-40	22.31	32.84	0.47
B2-N-40	23.80	34.49	0.45
B3-N-40	25.11	35.82	0.43

FIGURE 9   (A) Microscopic image of a triaxial braided structure with axial glass yarns. (B) The schematic of the triaxial braid cross-section

greatly improved the predicted results especially for the biaxial braids.

2. The cross-sectional of the braids were examined by a microscope. It was observed that the presence of axial yarns in the braided structure creates an empty space or void between the two layers of the braid (Figure 9A), which is not in the biaxial ones.

Therefore, in triaxial braided structures, it is necessary to insert a correction factor in the axial section. The schematic of the triaxial braid cross-section shown in Figure 9B, was considered and used to calculate the correction factor.

Where t_b, t_p, t_a, and t_v are the braid thickness, the yarn polyester thickness or diameter, the axial yarn thickness in braid structure due to outer layers, and the totally empty space length created, respectively. Therefore, tb is equal to the sum of $2 \times$ tp and the diameter of the axial

yarn calculated by Equation (9) which is one of the helpful equations to relate the linear mass or yarn count in den (mass of 9000 m) to its diameter:

$$\mathrm{den} = \frac{9\rho\pi D^2}{4000},\tag{9}$$

where ρ, is the linear density of yarn in grams per centimeter to the power of 2, and D is the yarn diameter in terms of micron.

The other parameters shown in Figure 9B were measured using microscopic images. Finally, the ratio of the area of the axial yarn to the area of the empty space created is calculated as the correction factor. The calculated values of the required parameters in terms of millimeter and the correction factor of the triaxial braided structures are listed in Table 4.

It should be noted that the braiding angle changes by applying force during a tensile test and this leads to a change in a braided structure. Therefore, the Krenchel factor is a different form and is the second power of cos the angle between the applied force and the supporting fiber. This was shown in some of the papers on braid structures.

Therefore, Equations (3) and (4) are modified, then Equations (10) and (11) are presented for biaxial and triaxial braids, respectively:

$$E_{11} = \cos^2\theta \times (V_{f1}E_{f1} + V_{f2}E_{f2}),\tag{10}$$

$$E_{11} = \left(\cos^2\theta \times V_{f1} \times E_{f1}\right) + \left(C \times V_{f2} \times E_{f2}\right)\tag{11}$$

and C is the correction factor.

The results of Equations (10) and (11) are compared with the experimental results in Table 5 and Figure 10.

As can be seen, the results obtained from the model are very close to the experimental values. Also, in all samples, the difference between the experimental and predicted values is approximately 2–3 N. Therefore, the proposed model can estimate the tensile modulus of tubular biaxial and triaxial hybrid braided structures with

TABLE 4 The obtained result

Braid code	Diameter of axial yarn (mm)	ta (mm)	tb (mm)	tp (mm)	tv (mm)	Correction factor
T-B-40	0.605	0.3	1	0.486	1.278	0.47
T-G-40	0.547	0.3	1	0.486	1.278	0.43

TABLE 5 The obtained result

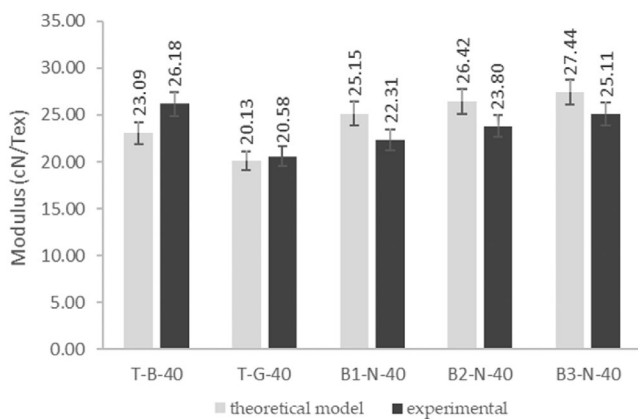| Braid code	The experimental value	The value obtained from the model	SD
T-B-40	26.18	23.09	0.12
T-G-40	20.58	20.13	0.02
B1-N-40	22.31	25.15	0.13
B2-N-40	23.80	26.42	0.11
B3-N-40	25.11	27.44	0.09

FIGURE 10 The tensile modulus results in tubular hybrid braid

a good accuracy. In the case of triaxial braids, basalt has been shown to perform better than glass. Considering that glass has negative effects on the environment, the use of basalt which is produced from volcanic rocks seems useful. Furthermore, this figure shows that a high functional yarn like basalt as axial yarns in the triaxial braid has a better tensile function than as braid yarns in the biaxial braid. However, in biaxial hybrid fabrics, the tensile properties increase with increasing basalt content.

5 | CONCLUSIONS

The mechanical properties of the yarns that made a braided structure cannot always be easily calculated without performing a destructive test. Therefore, in this paper, a model for predicting the tensile modulus of 2D hybrid tubular braided structures as the advanced fiber-reinforced composite materials were developed and proposed without any destructive tests for calibration. In this

model, a braided structure was considered a multilayer shell. Due to the different yarns used in the braided structure, the rules and equations used in the composite can be applied to the intended multi-layers.

In this work, the braided structures were not impregnated with resin, but different yarns were used for production. Due to the recognizability of the used yarns withinside the braided structures, the hybrid braid structure changed into taken into consideration as a composite material and the equations were developed. Since the modulus calculated in this way is in good agreement with the experimental results, the proposed model can be used as a suitable starting point for the development of other models about these structures. The hybrid braided compounds can be produced based on the present results to fulfill the desired properties of the manufacturer at a low cost. The concluded remarks confirmed that the use of basalt inside the braided preforms leads to a more tensile modulus of the braided preform, also an increase in the quantity of basalt will grow the tensile modulus of the braided preform to a more extent. This is due to a higher modulus of basalt compared to polyester. The presence of basalt in the braided structures as a high-overall performance yarn as an axial yarn in triaxial braided structures compared to biaxial ones and the use of the high-overall performance yarn as a diagonal yarn presents different outcomes. In biaxial hybrid braided preform structures, basalt and polyester are used as the diagonal yarn some instabilities to the peak point are eliminated by increasing the amount of basalt yarn. In triaxial braided preform structures, that used basalt and polyester as axial and diagonal yarns, respectively, there are several peaks with a value less than the prominent peak after the one. The overall performance outcomes put the triaxial braided preform structures in a better rank compared to the biaxial ones.

It should be noted that the good agreement between the theoretical and experimental results can be the promise that if the results of this work are used, there is no need to perform a destructive test.

ORCID

Ghazal Ghamkhar https://orcid.org/0000-0001-5593-0190

Mahdi Bodaghi https://orcid.org/0000-0002-0707-944X

REFERENCES

[1] V. Gribniak, A. P. Caldentey, G. Kaklauskas, A. Rimkus, A. Sokolov, *Eng. Struct.* **2016**, *124*, 418.

[2] R. Jakubovskis, G. Kaklauskas, V. Gribniak, A. Weber, M. Juknys, *J. Compos. Constr.* **2014**, *18*(5), 4014005.

[3] V. Gribniak, V. Cervenka, G. Kaklauskas, *Eng. Struct.* **2013**, *56*, 2175.

[4] V. Gribniak, G. Kaklauskas, L. Torres, A. Daniunas, E. Timinskas, E. Gudonis, *Compos. Part B: Eng.* **2013**, *50*, 158.

[5] D. Brunnschweiler, *J. Text. Inst.* **1954**, *45*(1), 55.

[6] S. L. Phoenix, *Text. Res. J.* **1978**, *48*(2), 81.

[7] K. Hristov, C. E. Armstrong, M. Dunn, C. Pastore, Y. Gowayed, *Text. Res. J.* **2004**, *74*(1), 20.

[8] A. Rawal, R. Kumar, H. Saraswat, *Text. Res. J.* **2012**, *82*(16), 1703.

[9] H. Dabiryan, M. S. Johari, *J. Text. Inst.* **2016**, *107*(5), 553.

[10] D. Boris, L. Xavier, S. Damien, *J. Ind. Text.* **2018**, *47*(8), 2184.

[11] Z. Yujing, M. Zhuo, D. Chengjie, Y. Linlin, S. Yize, *J. Eng. Fibers Fabr.* **2021**, *16*, 1558925021990483.

[12] M. Afzali Naniz, M. Bodaghi, M. Safar Johari, A. Zolfagharian, *Polymer* **2020**, *12*(3), 682.

[13] M. A. Naniz, M. S. Johari, *Mater. Res. Express* **2019**, *6*(11), 115315.

[14] H. Noughabi, M. Vadood, M. S. Johari, *Mater. Res. Express* **2018**, *5*(6), 65324.

[15] M. Ghaedsharaf, J. E. Brunel, L. L. Lebel, *Compos. Part B: Eng.* **2021**, *218*, 108938.

[16] A. Singh, Z. Gue, X. Hou, Y. Liu, D. J. Hughes, *Compos. Struct.* **2022**, *282*, 115107.

[17] M. Masoumi, H. Mansoori, T. Dastan, M. Sheikhzadeh, *Compos. Struct.* **2022**, *284*, 115231.

[18] J. Han, R. Wang, D. Hu, J. Bao, X. Liu, X. Guo, *Compos. Struct.* **2022**, *286*, 115309.

[19] W. Sun, C. Li, L. He, Z. Shan, X. Cheng, *Proc. Inst. Mech. Eng. C: J. Mech. Eng. Sci.* **2022**, *236*, 9544062211069314.

[20] X. Han, J. Zhang, H. Wang, W. Cui, D. Wang, *Proc. Inst. Mech. Eng. C: J. Mech. Eng. Sci.* **2021**, *235*(22), 6529.

[21] Y. Wang, Z. G. Liu, Y. P. Yi, Y. C. Wei, Z. Li, W. Yi-Bo, *Polym. Compos.* **2021**, *42*(4), 1912.

[22] Y. Sun, Y. You, W. Jiang, Q. Wu, B. Wang, K. Dai, *Appl. Mater. Today* **2020**, *18*, 100469.

[23] O. Eryilmaz, E. Sancak, *Polym. Compos.* **2021**, *42*(12), 6455.

[24] B. Shi, T. Wang, L. Shi, J. Li, R. Wang, J. Sun, *Appl. Mater. Today* **2020**, *19*, 100610.

[25] M. Arianpour, M. S. Johari, H. Dabiryan, *J. Text. Inst.* **2021**, *113*, 1.

[26] D. S. Li, W. F. Han, L. Jiang, *Compos. Commun.* **2021**, *28*, 100884.

[27] G. W. Melenka, A. Gholami, *Compos. Commun.* **2021**, *27*, 100813.

[28] S. R. Zahabi, M. Sheikhzadeh, S. Akbarzadeh, A. Bahi, F. Ko, *Polym. Compos.* **2022**, *43*(5), 3290.

[29] L. Gritsch, E. Perrin, J. M. Chenal, Y. Fredholm, A. L. Maçon, J. Chevalier, A. R. Boccaccini, *Appl. Mater. Today* **2020**, *22*, 100923.

[30] M. May, S. Kilchert, T. Gerster, *Materials* **2021**, *14*(17), 4890.

[31] M. Kolloch, G. Puchas, N. Grigat, B. Vollbrecht, W. Krenkel, T. Gries, *Materials* **2021**, *14*(21), 6338.

[32] ASTM International, *Standard Specification for Glass Fiber Strands*, ASTM International, West Conshohocken, PA **2018**.

[33] ASTM International, *Standard Test Method for Tensile Properties of Yarns by the Single-Strand Method*, ASTM International, West Conshohocken, PA **2002**.

[34] R. M. Jones, *Mechanics of Composite Materials*, CRC Press, Boca Raton **2018**.